# On the influence of a large scale coherent vortex on the turbulent cascade

F. Chillü, J.-F. Pinton, R. Labbé

# On the influence of a large scale coherent vortex on the turbulent cascade

**F. Chillà, J.-F. Pinton[1] and R. Labbé[2,3]**

[1]École Normale Supérieure de Lyon, Laboratoire de Physique, 46 allée d'Italie, F-69364 Lyon cedex 07, France
[2]École Normale Supérieure de Lyon, Laboratoire de Physique, 46, allée d'Italie, F-69364 Lyon cedex 07, France
[3]Present address: Universidad de Santiago de Chile, Casilla 307, Correo 2, Santiago, Chile

**Abstract.** We investigate the flow between coaxial co-rotating disks in the situation where a strong axial vortex is present over a turbulent background. This flow is nonstationnary and inhomogeneous as is commun in most turbulent geophysical flows. We describe the small scale statistics using tools recently introduced for homogeneous turbulent flows. It seems that the cascade process is preserved although modified by the large scale coherent structure.

## 1 Introduction

Apart from the fundamental problem of description of a non-linear dissipative system, one of the long standing goals of the study of *homogeneous turbulence* has been to derive tools that can be applied to solve the problems of *inhomogeneous turbulent flows* which have a wider practical importance. In the analysis of the flow field behavior, it has been customary since the works of Osborne Reynolds to represent the velocity of a high Reynolds number flows as the sum of two contributions:

$$\vec{v} = \vec{U} + \vec{u} \tag{1}$$

where $\vec{U}$ is the mean flow field – experimentally, it can be constructed by low-pass filtering $\vec{v}$ in space and time – and $\vec{u}$ are the turbulent fluctuations. In inhomogeneous flows, $\vec{U}$ is not constant in space and time and the question arises about the interaction and equilibrium between the large scale flow and the turbulent fluctuations. Such inhomogeneous 3D turbulent flows are common in geophysics. The present study is concerned with a flow in which a large scale coherent vortex is superimposed on a turbulent background. Such a flow has some characteristics of a moving tornado (high rotation rate at large scale together with turbulent three dimensional fluctuations).
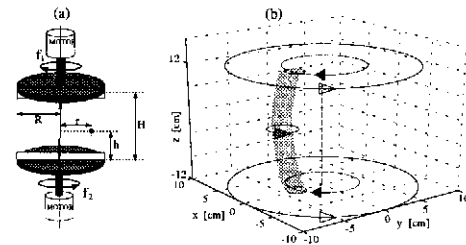


**Fig. 1.** (a) Experimental set-up. The working fluid is air. $R = 10$cm, $H = 30$cm. $f_1$ and $f_2$ are the disks rotation frequencies, and ($r = 7$cm, $h = 15$cm) are the coordinates of the hot-wire probe. (b) Contour plot of the velocity modulus $|v|(t)$ measured with a 3D hot-wire probe; it reveals the large scale coherent vortex (core size $\sim 2$cm; the rotation rates of the motors are equal to 11 and 43 Hz). The arrows indicate the directions of rotation of the disks, of the vortex and of its slow precession motion.

We analyze the influence of the vortex structure on the turbulence properties at small scales. The characterization is done using adapted forms of some of the most recent tools used in the study of homogeneous, isotropic turbulence. We do not attempt here to discriminate bewteen the different intermittency models that are currently being debated in the homogeneous turbulence community. However, we show using two examples that such models can be used in inhomogeneous turbulent situations and that they give some insight about the modification of the energy cascade by the presence of a large scale coherent structure.
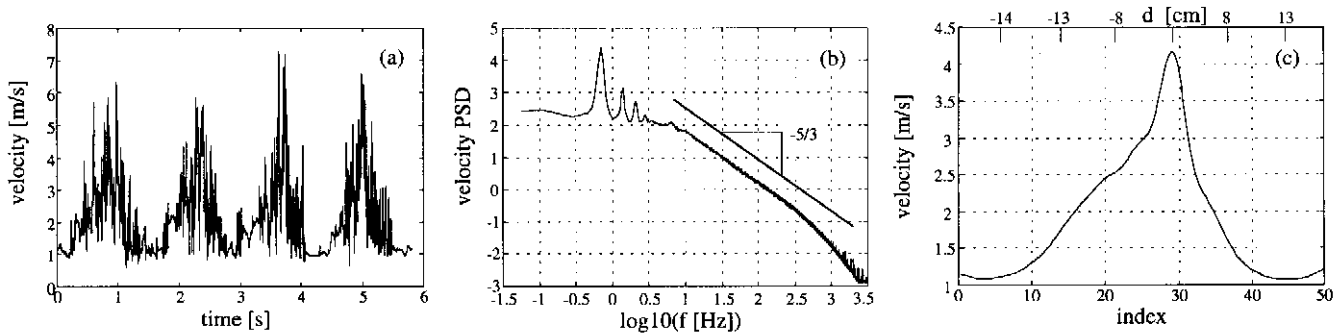
*Correspondence to:* J.-F. Pinton

**Fig. 2.** Low frequency evolution of the flow about the coherent vortex – $f_1 = 11\text{Hz}$, $f_2 = 43\text{Hz}$, $H = 30\text{cm}$. (a) : direct time-recording of the velocity at $h = 15\text{cm}$, $r = 7\text{cm}$. (b) Power Spectral Density of the velocity field (no coherent averaging). (c) : mean velocity profile during one oscillation as obtained by the coherent averaging process. The numbers on the lower x-axis correspond to an index in the subdivision of one period of the vortex precession motion. The corresponding distances to the vortex core are indicated on the upper x-axis.

## 2  Flow and Experimental set-up

The flow is produced in the gap between two coaxial corotating disks driven at regulated constant speeds, see fig. 1(a). Air is the working fluid, in a free geometry in order to eliminate side-wall effects. The detailed experimental set-up is described in Labbé et al. (1995) where it is also shown that when the disks are corotating at different angular speeds, the structure of the flow is made up of a large scale strong vortex superimposed to a turbulent background. The vortex has a Burgers type structure and is anchored on each disk at the point of maximum stretching. This point is not on the axis of rotation (as it would if the flow was enclosed in axisymmetric cylindrical walls); as a result the outgoing flow near the disk surface induce a slow, counter-rotating, precession motion of the vortex about the axis of rotation of the disks (Magnus force). This is illustrated in figure 1(b), where the vortex shape is reconstructed from 3D velocity measurement – again see the details in reference Labbé et al. (1995).

In our study, local velocity measurements are performed using a TSI subminiature hot-film probe with a sensing element $10\,\mu\text{m}$ thick and 1 mm long – the probe sensing element is set parallel to the rotation axis so that the velocity actually measured mixes the radial and azimuthal components $v = \sqrt{v_r{}^2 + v_\theta{}^2}$. The TSI IFA100 anemometer voltage is recorded using a National Instrument NB-MIO16-XL 16 bits data acquisition card. Velocities $v$ are derived from voltage data $E$ using the usual Kings law $\sqrt{(v)} = (E^2 - a)/b$, the validity of which has been checked and the constants $a$ and $b$ obtained from measurements in a calibrated wind tunnel. The independence of the result with the probe support position has also been checked.

An instantaneous velocity recording is shown in fig-

ure 2(a), where one observes the slow periodic sweeping of the vortex on the fixed anemometer probe, in addition to a very fluctuating velocity signal, resembling usual turbulent velocity variations. The two times scales are very different as may be seen on the corresponding power spectrum of figure 2(b). The low frequency precession motion, and its harmonics, are clearly identified as well as the typical turbulent Kolmogorov 5/3 scaling in the higher frequencies region. The large separation between the time scales allows to perform a Reynolds-like decomposition with a slowly evolving mean flow. To wit, we have used the coherent adaptive-averaging technique described in Labbé et al. (1995); Labbé, PhD Thesis (1996), first to extract the time-periodic mean flow due to the precession of the axial vortex, and second to characterize the statistical properties of the turbulent fluctuations at different phases of the mean-flow cycle. The main steps of the technique are the following: starting with a time recording like the one of figure 2(a), one calculates the mean period $T$ (about 3 seconds in our case) and then choses a model pattern (one burst of length $T$) and translate it to maximize the correlation with the next burst. The average of the two bursts is then calculated and serves as the model pattern for the next iteration. The process is self-adaptive and converges to the time recording of the mean flow cycle as shown in figure 2(c). The point of maximum average velocity corresponds to the passage of the vortex core, while the points of low mean velocity correspond to instants when the vortex is farthest from the probe. The fluctuation component is analyzed in the following way: the algorithm is re-run to identify and mark each individual oscillation by best correlation with the previously calculated averaged pattern, then each period is viewed as one realization of the turbulent flow about the vortex. If it is divided into subintervals then

ensemble averages can be calculated, conditioned to a particular phase of the mean flow. In the following, we have taken 50 subintervals; at the chosen sampling rate (30kHz), each interval holds 1200 points and the conditioning over 2300 periods of the vortex precession yields statistics calculated with about $2.4 \times 10^6$ data points. As the motion of the vortex is periodic in space, we can identify each subinterval with a particular (curvilinear) distance between the vortex and the anemometer probe, so that we analyze the structure of the turbulent fluctuations conditioned to the distance $d$ to the large scale vortex.

## 3 Results

### 3.1 General characteristics of the turbulent fluctuations

We first need some characterization of the turbulence intensity of the velocity fluctuations, conditioned to the distance $d$ to the vortex core. For lack of a real definition of a turbulent state, we resort to traditional analysis which suggests to consider the power density spectrum of the velocity fluctuations, the scale separation in the flow and the scaling properties of the velocity differences. Figure 3(a) shows the spectra of the velocity fluctuations for several values of $d$. As can be observed each curve display a $-5/3$ Kolmogorov scaling region. The range over which this scaling extends is limited due to the finite values of the Reynolds number in the flow. Indeed, a measurement of scale separation can be obtained by calculation of the Taylor microscale $\ell_T$ and Kolmogorov dissipation length $\eta$. Both quantities rely on an estimation of the energy dissipation $\epsilon$ in the flow. We have used the usual one-dimensional surrogate:

$$\epsilon(d) = 15\nu \frac{1}{U_d^2} \left( \frac{\partial u}{\partial t} \right)^2 \tag{2}$$

where $\nu$ is the air's kinematic viscosity and $U_d$ is the local average velocity. We use a local implementation of the Taylor hypothesis to relate space and time velocity derivatives (see Pinton et al. (1994)), in order to account for the advection of the turbulent fluctuations by the large scale velocity variations. The results show that the dissipation is maximum about the vortex core. The scales $\ell_T$ and $\eta$ are then calculated as follows (see Monin & Yaglom (1971)):

$$\frac{1}{U_d^2} \left( \frac{\partial u}{\partial t} \right)^2 \sim \frac{u_{rms}^2}{\ell_T(d)^2} , \tag{3}$$

and,

$$\eta(d) = \left( \frac{\nu^3}{\epsilon(d)} \right)^{1/4} . \tag{4}$$

The variation of $\eta(d)$ is displayed in figure 3(b). Assuming an integral scale $L$ of the order of a few centimeters

(order the size of the coherent vortex and of the blades fitted on the disks), one anticipates an inertial range of the order of one decade at most. To compare this with traditional, homogeneous turbulence measurements, we calculate the local Reynolds number $R_T$ based on the Taylor microscale and the intensity of the turbulent velocity fluctuations:

$$R_T = \frac{u_{rms}\ell_T}{\nu}. \tag{5}$$

As can be observed in figure 3(c), $R_T$ varies in the range 70 to 350, where a decade of inertial range at best may be expected. To wit, we study the scaling of the third order structure function, which, according to the Kármán-Howarth relationship, traditionally defines the inertial range. In our case the statistical ensemble is not large enough to calculate accurately the odd moments of the velocity increments; in the wake of some recents works (see Benzi et al. (1993, 1995b)) we use for odd moments the absolute value of the velocity differences, i.e. for the third moment:

$$F_3(r) = < |v(x + r) - v(x)|^3 >_x \tag{6}$$

There is some evidence (for example Benzi et al. (1995a)) that this quantity gives the same information as the actual third order structure function. Figure 3(d) shows a plot of $F_3(r)$ conditioned to a few values of $d$. A clear inertial range is observed, whose extent increases closer to the vortex core. This in agreement with our previous observations, e.g. the spectra of figure 3(a) and the decrease of $\eta$ in figure 3(c). It also agrees with traditional homogeneous turbulence results: in the neighborhood of the vortex $R_T$ increases so that the range of self-similar scales is widened.

The picture we get from this first analysis is the following: at every step of the flow cycle, i.e. for each distance to the coherent vortex, the flow is locally turbulent. Our results seem to be locally in agreement with homogeneous turbulence measurements. We note that this local assumption of homogeneous, isotropic turbulence is often used in numerical simulations of flows that are inhomogeneous at large scales (examples include meteorology, aircraft engineering, etc.). In such cases, the effects of the small scale turbulence are taken into account using local variables only (L.E.S., $k - \epsilon$ model). Our aim here is to go one step beyond and investigate the possible influence of the inhomogeneity of the flow at large scale on the structure of the energy cascade. This is a natural question to ask in flows where the scale separation is limited, as in many practical situations. We then need to analyze the flow using tools that are particularly sensitive to finite Reynolds number effects. Such techniques have recently been developed for the study of homogeneous, isotropic turbulence. In the following we use two frameworks: one, based on the study of the modification of the PDFs of velocity increments with scales, proposed by B. Castaing and the Extended Self
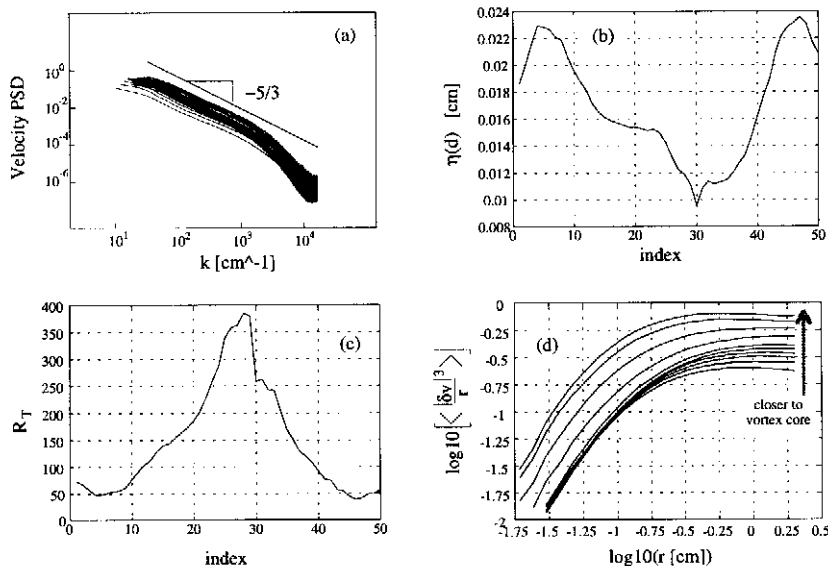
**Fig. 3.** (a) PSD of the velocity fluctuations conditioned to the values of $d$, the straight line materializes the Kolmogorov $-5/3$ slope; (b) Kolmogorov dissipation length $\eta(d)$; (c) turbulent Reynolds number $R_T$ based on the Taylor microscale; (d) evolution of the compensated third moment $F_3(r)$, as one gets closer to the vortex core (indices 18 to 28).

Similarity (ESS) analysis as proposed by R. Benzi and co-workers. We emphasize again that our goal is not to discriminate between different intermittency models of homogeneous turbulence (it would not be possible here) but to show how a large scale coherent structure influences the energy cascade at small scales. For this purpose we have used two convenient techniques and obtained coherent results.

## 3.2  PDF description, Castaing's model

It has become customary to study the energy cascade through the behavior of the longitudinal velocity increments $\delta u_r = \vec{e}.[\vec{u}(\vec{x} + r\vec{e}) - \vec{u}(\vec{x})]$. For homogeneous turbulence situations, it has been proposed by Castaing at al. (1990) and confirmed experimentally by Gagne et al. (1994) that the Probability Density Function (PDF) of $\delta u_r$ may be reconstructed as a superposition of functions having the shape of the integral scale statistics $P_L$ and a range of width $\sigma$:

$$P_r(\delta u) = \int G_{rL}(\ln \sigma)\frac{1}{\sigma}P_L\left(\frac{\delta u}{\sigma}\right) d\ln \sigma \qquad (7)$$

where $G_{rL}$ is the distribution function of $\ln \sigma$, with characteristic width $\lambda_r^2 \equiv < (\Delta \ln \sigma)^2 >$. Indeed, $\lambda_r^2$ grows as the cascade proceeds to finer scales and thus gives a measure of the deepness of the turbulent cascade; the way it varies with scale $r$ thus provides a description of the intermittency phenomenon. For example, the Kolmogorov (1962) intermittency corrections are recovered if one assumes a lognormal distribution of $\ln(\sigma)$.

In the original formulation of the Castaing's approach $\lambda_r^2$ was obtained from direct fit of the PDFs $P_r(\delta u)$ with a superposition of Gaussian statistics. Here, we use a recent result of Castaing (1996) showing that in the range of scales where the cascade is self-similar the distribution function $G_{rL}$ is an infinitely divisible one, and $\lambda_r^2$

may be easily computed from the kurtosis $K$ of $P_r(\delta u)$ (see Chillà et al. (1996)):

$$\lambda_r^2 = D \ln \frac{K}{K_L} \qquad (8)$$

In the above expression $K_L$ is the kurtosis of the large scale distribution $P_L$ and $D$ is a proportionality constant whose expression depends on the intermittency model and weakly on the Reynolds number (numerically, one finds $D \sim 0.3$ in most laboratory experiments studying homogeneous isotropic turbulence). We note that equation (8) provides an efficient calculation of $\lambda_r^2$ and does not make any particular assumption about the PDFs' skewness as discussed in Castaing (1996). We thus proceed to the calculation of the behavior of $\lambda_r^2$, conditioned to the cycle of the coherent large scale vortex motion.

Figure 4(a) shows the PDFs of velocity differences, for different values of $r$, at 7.6cm to the vortex core and figure 4(b) shows the corresponding $\lambda_r^2$ curve. It is observed that the intermittency increases at small scales and that one can identify a scaling region:

$$\lambda_r^2 \propto r^{-\beta} \qquad (9)$$

for $r \in I \equiv [\ell_1, \ell_2]$. We want to stress that what is tested here is the way the intermittency grows when going to smaller scales. In particular, the scaling interval $I$ defined above differs from the inertial range interval considered in the previous section. Indeed, it can be shown (see Castaing (1996)) using equation (7) that $\ln < \delta u_r^p > \propto \lambda_r^2$, so that a power law behavior of the velocity increments cannot be observed in the interval of scales $I$. However, the $r^{-\beta}$ behavior of $\lambda_r^2$ is firmly established in homogeneous turbulent flows at moderate to high Reynolds numbers (Castaing at al. (1993); Chabaud et al. (1995)). That it is observed here in the
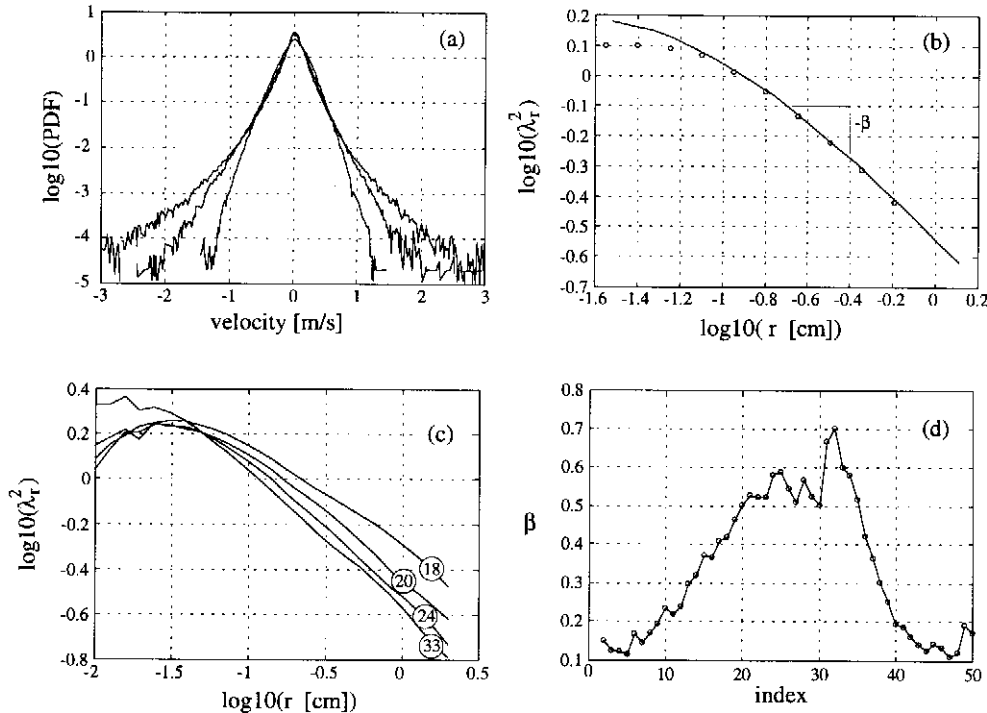
**Fig. 4.** (a) Probability Density Function of the velocity differences $\delta v_r$ at index 23 (7.6 cm from the vortex core). The curves are calculated for $r$ =0.03 cm (inner curve), 0.16 cm and 0.91 cm (outer cuve); (b) corresponding curve $\lambda_r^2$. The solid line is calculated using the PDFs kurtosis (and $K_L = 3$), the circles are obtained using a best fit based on equation (2) as in reference Castaing at al. (1990); (c) Examples of $\lambda_r^2$ curves conditioned to the proximity to the vortex core: $d = 10.3, 9.2, 4.4, 4$cm, correspondng to indices 18, 20, 24, 33 respectively. (d) Values of $\beta(d)$ calculated at all phases of the coherent vortex motion.

presence of a large scale coherent structure is encouraging as to the capacity of the model to describe the intermittency in more complex flows.

We now proceed with calculations conditioned to the proximity to the large scale vortex. Figure 4(c) shows the $\lambda_r^2(r)$ curves at distances $d$ =4.4,9.2 and 10.3cm before the vortex and 4cm after. An almost linear region in $\ln(\lambda_r^2)$ $vs$ $\ln(r)$ coordinates can be found at each distance to the vortex, indicating again a power law behavior but with a varying slope. Figure 4(d) shows that $\beta$ increases closer to the vortex core. This can be explained if one interprets the curves in the following manner: *(i)* at small scales the value of $\lambda_r^2$ are almost the same for each $d$, i.e. the intermittency at small scales is little affected by the vortex (as much as the variations of $\eta$), *(ii)* in the large scales the values of $\lambda_r^2$ decreases with $|d|$, showing the effect of the coherent structure; as a result $\beta$ increases as one gets closer to the vortex core. This description is in agreement with the expected effect of a large vortical motion. However, this behavior is different from what is observed in homogeneous turbulent flows, where $\beta$ decreases with increasing Reynolds numbers (Chabaud et al. (1995)) – remember that $R_T$ increases close to the vortex.

An attempt to solve this apparent contradiction may be done using for $\beta$ the following expression

$$\frac{1}{\beta} \propto \ln \frac{L}{\eta} \qquad (10)$$

where $L$ is the integral length scale and the Kolmogorov dissipative length. In the turbulent flows, $L/\eta \sim Re^{-3/4}$,

so that the observed $1/\beta \sim \ln(Re)$ law is recovered. In the turbulent flow near the vortex, $\eta$ decreases (see figure 3(c)), but at the same time so does $L$. Assume, then, that the local effective integral length scale at distance $d$ is equal to $d$ itself. Furthermore, the variations of $\eta e^{-3/4}$ are much smaller than the variations of $L \sim d$, so that $L/\eta$ actually decreases with $d$. This "rescaling" of the integral length scale by the proximity of the coherent vortex gives the correct trend for variations of $\beta(d)$. However, a plot of $\beta \ln(d/\eta)$ as in figure 5 does not reveal a trivial behavior. Finally, we note that it would possible to redefine the integral scale $L$ in order to enforce the validity of equation (10). With the measured variations of $\beta$ it would lead to very large values of $L$ at large distance from the vortex; such a behavior cannot be ruled out since the flow is not confined.

As a partial conclusion, we observe that the above framework yields a description of the local intermittency. However, the results show some difference with homogeneous turbulence analysis and seem to indicate that global structure of the flow may thus be of importance, so that the energy cascade is modified by the proximity of the coherent structure. To check this findings we have analyzed our data using a different framework, based on the Extended Self Similarity ansatz.

### 3.3 Extended Self Similarity

It has been observed by Benzi et al. (1993), in the case of isotropic homogeneous turbulence, that the scaling range of the velocity increments structure functions can
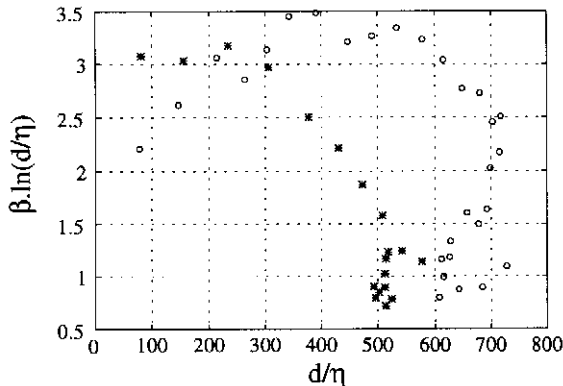
**Fig. 5.** Values of $\beta(d)$, renormalized by taking an effective integral length scale equal to the distance to the vortex core: (o) before and ($*$) after the passage of the vortex.

be greatly extended when they are plotted one against the other. More specifically, extending the Kármán-Howarth relationship to use the third order structure function as a surrogate for the scale $r$, one observes the scaling:

$$< |\delta u_r|^p >\propto< |\delta u_r|^3 >^{\xi_p} \tag{11}$$

over a very wide range of scales, from integral length scale $L$ to a few times the dissipative Kolmogorov length. In addition, the exponents $\xi_p$ are identical to the usual structure functions exponents $\zeta_p$. This property, has been widely used (see Arnéodo et al. (1996)) to calculate the values of $\zeta_p$ in flows at moderate turbulent Reynolds numbers $R_\lambda$. Recently, it has been shown that the ESS property can be obtained as a consequence of infinite divisibility assumption for the turbulent cascade (She & Waymire (1995); Castaing (1996)).

We have thus calculated the structure functions exponents $\zeta_p$ using the ESS ansatz, conditioned to the distance to the vortex. As in homogeneous turbulent flows, the 'local' structure functions exhibit the ESS property for a range of scale varying between a few Kolmogorov lengths and the effective integral scale (in the conditioning procedure the motion of the vortex is divided in subintervals, so that the largest scale in each interval is roughly 2 cm). The corresponding exponents are reported in figure 6(a). Note that we have plotted the intermittency corrections $\zeta_p - p/3$, which is the difference between the observed structure function exponent and the Kolmogorov $p/3$ predicted values. We observe that they vary by over 30% during one cycle of the coherent vortex motion, with systematic trends: as one approaches the vortex core the exponents get closer to their K41 value ($\zeta_p \to p/3$) showing that the intermittency is reduced. This is in agreement with our findings of the previous section.

However, some unusual behavior has been found in other inhomogeneous flows, as in presence of a large

shear as shown by Benzi et al. (1995b) (ESS not working at all) but the self scaling behavior was recovered using a generalized version of the ESS ansatz. Indeed it was shown in these cases that a 'universal' behavior of the exponents was recovered if one considered their relative variations. More precisely, it was shown that the so-called generalized exponents:

$$\rho(p,q) = \frac{\zeta_p - p\zeta_3/3}{\zeta_q - q\zeta_3/3} \tag{12}$$

had identical values in a very wide variety of flow situations. We have thus computed the value of $\rho(4,2)$, conditioned to the distance to the vortex core. As can be observed in figure 6(b) it is not constant (it varies by a factor of 2!), although the average over the entire vortex motion has the 'universal' (-1.58) value proposed by Benzi et al. (1995b).

This study shows again that the turbulent cascade is modified in the vicinity of a large scale coherent vortex: the intermittency decreases as one gets closer to the vortex core.

## 4  Conclusion

We have shown that the tools recently developed for the analysis of the turbulent cascade in homogeneous flows can be applied to inhomogeneous anisotropic ones, at least when the large scale inhomogeneous flow consist of a single coherent vortex. It should be noted that in such condition with finite Reynold numbers, the traditional analysis (such as presented in section 3.1) is not sensitive enough to detail the influence of the large scale structure on the turbulent fluctuations. Finer approaches are based on a direct description of the cascade process. They reveal that the self-similarity of the cascade is preserved although strongly modified by the presence of the coherent structure. It is not clear at present if the observed modifications can be modeled by variations of the usual parameters of homogeneous turbulence alone. Some additional parameters describing the overall geometrical structure of the flow may be needed. Further investigations with coherent structures of different generic shapes (eg. a plane shear) are underway.
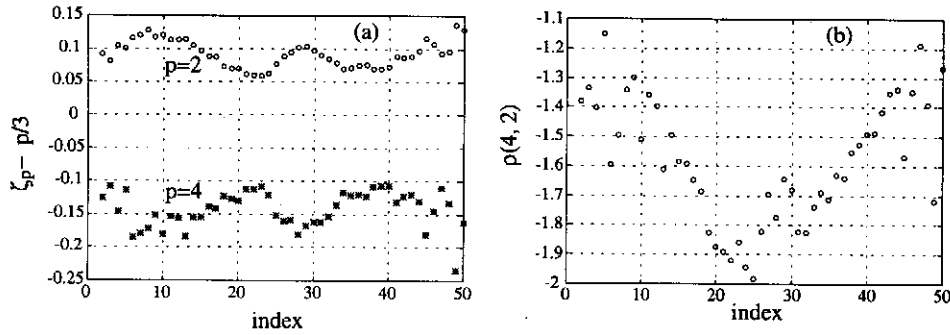
**Fig. 6.** (a) Structure function exponents (expressed as their difference with Kolmogorov value) at all phases of the coherent vortex motion. (o): 2nd order and (∗): 4th order. (b) corresponding generalized exponent $\rho(4, 2)$ – the mean value is -1.58.

# References

Labbé R., Pinton J.-F., Fauve S., *Phys. Fluids*, **8**(4), 914-922, (1996).

Labbé R., Thesis, E.N.S.Lyon, unpublished, (1996)

Pinton J.-F., Labbé R., *J. Phys. II France*, **4**, 1461-1468, (1994).

Monin A.S. , Yaglom A.M., *Statistical Fluid Mechanics*, MIT Press, (1971).

Castaing B., Gagne Y. and Hopfinger E.J., *Physica D*, **46**, 177-200, (1990).

Castaing B., Gagne Y., Marchand M., *Physica D*, **68**, 387-400, (1993).

Castaing B., *J. Phys. II France*, **6**, 105-114, (1996)

Chillà F., Peinke J., Castaing B., *J. Phys. II France*, **6**, 455-460, (1996).

Chabaud B., Naert A., Peinke J., Chillà F., Castaing B. and Hébral B., *Phys. Rev. Lett.*, **73**, (1994).

Gagne Y., Marchand M. and Castaing B., *J. Phys. II France*, **4**, 1-8, (1994).

Kolmogorov A.N., *J. Fluid Mech.*, **13**, 82-85, (1962).

Benzi R., Ciliberto S., Baudet C., Ruiz Chavarria G. and Tripiccione R., *Europhys. Lett.*, **24**(4), 275-279, (1993).

Benzi R., Ciliberto S., Baudet C., Ruiz-Chavaria G., *Physica D*, **80**, 385-398, (1995).

Arnéodo A. et al. *Europhys. Lett.*, **34**(6), 411-416, (1996).

She Z.S., Waymire E.C., *Phys. Rev. Lett.*, **74**, 336, (19965).

Benzi R., Biferale L., Ciliberto S., Struglia M.V., Tripiccione R., *Europhys. Lett.*, **32**, 709, (1995).